Journal of
Renewable Energy Research and Applications (RERA)

Vol. 3, No. 1, 2022, 79-92 *DOI: 10.22044/rera.2021.11130.1075*

Determining Optimal Arrangement of Distributed Generations in Microgrids to Supply Electrical and Thermal Demands using Improved Shuffled Frog Leaping Algorithm

Sh. Momen, J. Nikoukar* and M. Gandomkar

Department of Electrical Engineering, Islamic Azad University, Saveh branch, Saveh, Iran.

Received Date 22 August 2021; Revised 18 September 2021; Accepted Date 22 November 2021
**Corresponding author: j_nikoukar@iau-saveh.ac.ir (J. Nikoukar)*

Abstract
Global warming, environmental pollution, decreasing fossil fuels, increasing demand, and prices of energy carriers within the social and political conflicts between different nations are some of the problems for the traditional energy production and economic dispatch. In the traditional generation systems, about 25% of energy is wasted, and the presence of Distributed Energy Resources (DERs) such as Photovoltaic (PV), Wind Turbine (WT) and wind farms, Fuel Cell (FC), and Combined Heat and Power (CHP) can reduce fuel consumption, pollution, transmission losses, and increase in the micro-grid productivity. In this paper, a complete energy management framework in a micro-grid is proposed by considering the load distribution constraints using the Improved Shuffled Frog Leaping Algorithm (ISFLA) algorithm, in which it determines the exact share of energy production or consumption for different units. The proposed scheme is used to select the best arrangement of DERs in the power grid, by which the output is to determine the number and optimal location of DERs in the several bus-bars of the grid. Then the Independent System Operator (ISO) determines the quantity of energy exchange and consumption by considering the load distribution constraints. Boilers and CHPs are also used to maintain the balance between the production of thermal power by the energy sources and thermal demands. In addition, the Demand Response Program (DRP) is used with the aim of smoothing the load curve and reducing the operating costs. Finally, the proposed method is implemented and simulated on the IEEE 69 and 118 bus systems using the MATLAB software, which compares the output results with the existing algorithms, showing the superiority of the proposed method.

Keywords: *Demand Response, Energy Market, Optimization, Distributed Energy Resources, Improved Shuffled Frog Leaping Algorithm.*

1. Introduction

In the optimal planning and operation of micro-grids (MGs), there should be at least one applicable program for power generation management in the demand side and the available considered Distributed Energy Resources (DERs). According to [1], due to the increase in the greenhouse gas emissions and the concerns about the health of the global community and environmental pollution, the tendency to use renewable energies is growing. In [2], an applicable approach due to power consumption and MG energy management optimization has been investigated, which includes Demand Response Program (DRP) implementation for an MG operation in the grid-connected mode. The effect of using DRP in the daily MG production planning along with flattening the power profile and preventing the blackouts and postponing investment in the network in the island operation has been investigated [3]. The optimal implementations of economic programs to manage the DER productions in the grid-connected mode with the ability to exchange the power have been studied in [4]. In order to maximize the profits in the MG operation and increase the social welfare by considering the thermal loads, energy storage sources (ESSs) and the main network along with flattening the demand curve in a competitive market, some applicable DRPs have been utilized in [5, 6]. A two-stage stochastic programing has been used for DERs to participate in supplying the load by considering DRPs as a reserve [7]. In this study, in critical moments such as the transmission line outage, due to the generated reduced power, DRP has been applied to the participants as a piece-

wise linear program and mandatory shedding. The authors have used the mixed integer programming (MIP) method for DER planning, in which the producers and consumers can offer their biddings in five different blocks, which will increase the consumer profits and is able to reduce the market power [8].

According to the guidelines of the regional power companies, reducing the loads during peak intervals results in reducing the cost of economic load dispatch (ELD), and prevents high prices. Correspondingly, the hourly consumption pattern variations lead to a significant reduction in the local marginal price (LMP). In addition, DRP can smoothen the load profile curve, and either helps to reduce the operating costs or reduce the detrimental effects of carbon dioxide emissions. The security constraint unit commitment (SCUC) is a superior way to overcome ELD and reduction of the operating costs because SCUC contributes significantly to the flexibility and efficiency of the electricity market. Implementing DRP in the network has been modeled by the real-time pricing program in the presence of electricity price uncertainty, which has been conducted out through robust scheduling [9]. The operation planning has then been modeled along with the network security constraints with the impact of risk in the presence of WT [10]. In [11], the model proposed in [9] has been presented and solved by linearization that has been easily implemented. The concept of price dependence approach has been considered in many literatures including [12]. The elasticity and flexibility of the load concerning price can be defined in the ratio of the relative changes in load to the close modifications in price. In [13], the intermittent DRP has been studied as one of the most essential and common DRPs to minimize the costs. Price elasticity in [14] has been divided into two types of self and mutual groups. Self-elasticity is related to the loads that cannot be moved from one hour to the next such as light loads, in which case the value of this coefficient of elasticity is always negative. The coefficients of mutual elasticity, in turn, take positive values, and are attributed to the loads that can be delayed [15]. In [16], a comprehensive model has been presented, in which the dependence of load on the price has been shown through four functions: linear, potential, exponential, and logarithmic approaches. Then by acquiescing the weight coefficients to each one of the four functions mentioned, a comprehensive model of all these functions has been obtained. This paper noted that the most appropriate solution for the load functions was obtained by considering the price in the linear elasticity model. The Shuffled Frog Leaping Algorithm (SFLA) has recently been widely used in order to optimize energy consumption in MGs. The SFLA algorithm is based on a strategy related to meta-heuristic memetics [17]. The memetic algorithm is a population-based one used for difficult and significant optimization problems. The main idea of this algorithm is to apply a local search method within the structure of the genetic algorithm to improve the performance of the search intensification process. The memetic algorithm first encrypts the set of initial answers and then the algorithm calculates the suitability of each solution based on a fitness function and generates new responses [18]. The SFLA algorithm is inspired by how frogs search for food. The SFLA algorithm uses a combination strategy, and allows the exchange of messages in a local search. This algorithm combines the advantages of the anemometric algorithm and the particle group optimization. In the SFLA algorithm, the messages are exchanged not only in a local search but also in a global search. Thus the local and international searches are well-combined in this algorithm. SFLA is a high potential for the global search algorithms, and implements them efficiently. The SFLA algorithm can solve many non-linear, undetectable, and multi-state problems [19].

In this paper, using the improved SFLA, the most appropriate possible arrangement for DERs to reduce the operating costs in MG has been studied. The process is that first, the cost of all small-scale power plants is expressed according to their operating constraints, and then the improved SFLA is improved by selecting more favorable paths than before. In the next step in the IEEE standard systems, the best arrangement that DERs may be placed in different load capacities to maximize operating profit will be selected, and at the end, the network reliability indicators will be evaluated.

2. Problem Formulation

Figure 1 shows the structure of an MG that interacts with the electricity market. As it can be seen, the system under study includes the wind turbine units, solar units, fuel cells (FCs), batteries, DC/AC converters and loads (such types of loads including interruptible load, and non-interruptible load are also considered). This paper aims to determine the optimal number of DERs in MG provided that the total cost is minimized. In this regard, first, the prices of each production unit will be described.

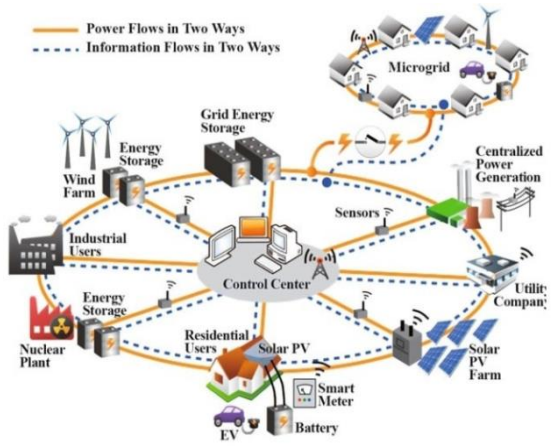

Figure 1. An MG considering DER exchanging energy with upstream network.

2.1. Solar unit model

The data related to the power reflected on the surface of the array is converted to its output power using equation 1.

$$\mathbf{P_{PV}} = \frac{\mathbf{G}}{\mathbf{1000}}\mathbf{P_{PV,rated}}\boldsymbol{\eta}_{\mathbf{PV}} \quad (1)$$

In this equation, G is the radiant power perpendicular to the surface of the array (W/m^2), and $P_{PV,rated}$ is the nominal power of each array obtained per 21,000 W/m^2. η_{PV} is also equal to the efficiency of the DC/DC converter installed between each array and the DC bus. If the vertical and horizontal components of the sun's radiant power are available at any given moment, the radiated power (vertically) on the surface of the array installed with the Θ_{PV} angle can be calculated according to equation 2 [20].

$$\mathbf{G(t,\theta_{PV})} = \mathbf{G_V(t)\cos(\theta_{PV})} + \mathbf{G_H(t)\sin(\theta_{PV})} \quad (2)$$

Where $G_H(t)$ and $G_V(t)$ are the horizontal and vertical radiation rates in my time step (W/m^2), respectively.

2.2. Wind turbine model

The power-velocity characteristics of the wind turbine used in modeling this work are given in reference [21]. This curve is usually provided by the turbine manufacturer, and expresses the actual power transmitted from the turbine to the DC bus. The output power (P_{WT}) in terms of wind speed (v_W) of this turbine can be approximated by equation 3, where v_{cutin}, v_{cutout}, and v_{rated} are the low cut-off speeds, high cut-off speed, and nominal speed (m/s) of the turbine, respectively, and $P_{WT,max}$ is the maximum output power of the turbine (kW), and P_{furl} is the output power at high cut-off speed. In this work, m is considered to be equal to 3.

$$P_{WT} = \begin{cases} 0 & ;v_w \le v_{cutin}, v_w \ge v_{cutout} \\ P_{WTmax} \times \left(\frac{v_w - v_{cutin}}{v_{rated} - v_{cutin}}\right)^m & ;v_{cutin} \le v_w \le v_{rated} \\ P_{WTmax} + \frac{P_{furl} - P_{WTmax}}{v_{cutout} - v_{rated}} \times (v_W - v_{rated}) & ;v_{rated} \le v_w \le v_{cutout} \end{cases} \quad (3)$$

The output power fluctuations of wind turbines caused by changes in wind speed are neither completely random nor entirely predictable. For an extended operation of a wind farm, the prediction error is like a normal distribution function. In order to reduce the risk of forecast error in system planning, we can calculate the forecast error at different levels of reliability. The forecast error of wind energy production is known as the production risk. For example, a 95% confidence level says that the probability that the forecast error is greater than the amount of production risk is less than 5%. This method is used in this work to wind energy capacity with a certain level of reliability in the production planning. The predicted wind energy minus production risk is the amount of power that should use in system planning. Since the planners are more inclined to overestimate the production of wind turbines, a one-way distribution curve is considered in this work. The following equations estimate the level of error above the one-way curve of the normal distribution with a confidence level of (100-α)%.

$$\mathbf{e'} = \boldsymbol{\mu}_\mathbf{e} + \mathbf{z}_\boldsymbol{\alpha}\boldsymbol{\sigma}_\mathbf{e}$$
$$\mathbf{P}(\mathbf{e} - \boldsymbol{\mu}_\mathbf{e} > \mathbf{z}_\boldsymbol{\alpha}\boldsymbol{\sigma}_\mathbf{e}) = \frac{\boldsymbol{\alpha}}{\mathbf{100}} \quad (3)$$

In the above equations, e' represents the production risk, μ_e is the mean wind forecast error, and σ_e is the standard deviation of the standard wind forecast error. In fact, $e'$is a value that says that the probability that the prediction error is higher than e' is less than %α. Thus according to equation 4, this can be shown.

$$\mathbf{P}(\mathbf{e} < \mathbf{e'}) = \mathbf{5}\,\% \quad (4)$$

Using the values of the mean error, standard deviation, and z_α, the production risk (e') is calculated from the previous equations, and the number obtained is subtracted from the predicted value, and this is the number that is entered as the output of the wind generator in the optimization problem.

2.3. Electrolyzer model

Electrolysis is the process of using electricity to split water into hydrogen and oxygen. Thus a

direct current of electricity passes through the path between two electrodes immersed in water, and causes the water to decompose into oxygen and hydrogen. Oxygen is produced on the cathode side and hydrogen on the anode side. Hydrogen is usually made at a pressure of about 30 bars. In order to generate electricity in a PEM fuel cell, it is sufficient for the pressure of the reactants to be 1.2 Bar (about slightly higher than the air pressure). However, increasing the density of the stored hydrogen sometimes increases its pressure by up to 200 bar [23]. Similarly, two storage tanks are used to reduce the energy required to compress hydrogen. The output of the electrolyzer is connected directly to the first tank after filling the first tank, the compressor is turned on, and then the hydrogen inside this tank is considered and will be filled into the second tank, which is called the high-pressure tank. This process will avoid the compressor running consecutively, and consumes less energy overall. In the proposed model of this work, due to the use of proton membrane fuel cell (PEM) and with considering that type of cell, the required hydrogen pressure is 1.2 bar. The compressor-free design reduces the energy consumption although the software developed is very flexible and the compressor model can be easily added to process. The electrochemical interactions in the water electrolyzer are as follows (5):

$$\mathbf{H_2O \rightarrow \frac{1}{2}O_2 + 2H^+ + 2e^-} \tag{5}$$

In the electrolyzer modeling, the efficiency is used as an input parameter. The hydrogen heating value is 3.4 kWh/m^3, which considering the efficiency of 90%, consumes 41.97 kWh of energy for the electrolyzer to produce one kg of hydrogen according to the following equation:

$$\mathbf{E_{cons} = \frac{\frac{3.4}{0.09}}{0.9} = 41.97 \frac{kWh}{kg}} \tag{6}$$

The weight of hydrogen produced per hour is obtained by dividing the excess energy produced from the system to the electrolyzer by 41.97.

$$\mathbf{H_2 = \frac{E_{gen}(kWh)}{41.97\left(\frac{kWh}{kg}\right)}} \tag{7}$$

2.4. PEM fuel cell model

Fuel cells are electrochemical devices that convert the chemical energy directly into the electrical energy. PEM cells have a reliable operation under discontinuous operating conditions, and are industrially produced on a large scale and commercially available. This type of fuel cell is suitable for large and in-situ applications, and has a relatively fast dynamic response, about 1 to 3 s. Therefore, in this work, a PEM type fuel cell is used. The output power of this fuel cell can be calculated as a function of the hydrogen power input to it and its efficiency (η_{FC}), which can be assumed to be constant [24].

$$\mathbf{P_{FC-inv} = P_{tank-FC}\eta_{FC}} \tag{8}$$

2.5. Hydrogen tank model

The energy that is stored in the tank can be calculated for each time step from equation 9.

$$\mathbf{E_{tank}(t) = E_{tank}(t-1) + P_{elec-tank}\Delta t - P_{FC-tank}\Delta t/\,\eta_{storage}} \tag{9}$$

In this equation, Δt is the length of each time step, $P_{elec-tank}$ shows the transfer power from the electrolyzer to the hydrogen tank, and $P_{FC-tank}$ represents the transfer capacity from the hydrogen tank to the fuel cell; $\eta_{storage}$ also represents the efficiency of the storage system, which can indicate the leakage or pumping losses. The maximum quantity of hydrogen stored in a tank is considered equal to its nominal capacity. It is also assumed that not all the stored hydrogen in the tank can be extracted due to some problems including the pressure drop inside the tank. The hydrogen in the tank will always have a high and low range.

$$\mathbf{E_{tank}(t)^{min} < E_{tank}(t) < E_{tank}(t)^{max}} \tag{10}$$

2.6. Battery model

The battery source is used in order to supply the load in the absence of the renewable energy sources. The difference between the power produced and the power required by the load indicates whether the battery should be charged or discharged. The amount of battery bank charge in the time period t is obtained using equation 11, which in the above relation $E_{bat}(t-1)$ and $E_{bat}(t)$ represents the amount of battery bank charge in the time periods (t-1) and (t); η_{bat} and η_{dis} are the charge and discharge efficiency of the battery bank, respectively.

$$\mathbf{E_{bat}(t) = E_{bat}(t-1) + P_{gen}\,\Delta t\,\eta_{bat} - P_{bat-inv}\Delta t/\,\eta_{dis}} \tag{11}$$

2.7. CHP model

According to the efficiency and load percentage in CHP, the power thermal can be approximated in piecewise linear (Figure 2). Given that only one part of the approximated graph can be used in

each interval, for modeling pure power and achieve that propose, we will have:

$$\mathbf{P^{CHP}} = \sum_{t=1}^{T} \sum_{j=1}^{N_{CHP}} \gamma_e^{CHP} * P_{t,j}^{gas(CHP)} \quad (12)$$

$$P_{t,j-1}^{elec(CHP)} * k_{t,j}^{CHP} < P_{t,j}^{CHP} < P_{t,j}^{elec(CHP)} * k_{t,j}^{CHP} \quad (13)$$

$$\sum_{j=1}^{N_{CHP}} k_{t,j}^{CHP} = 1 \quad (14)$$

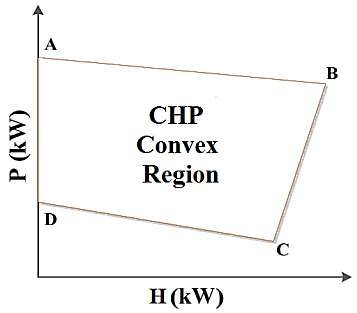

Figure 2. Available and convex area in CHP electrical and thermal output powers.

In the above equations, γ_e^{CHP} is the percentage of the electric power generated from the heat received. The rest of the energy will be converted to heat, which will provide thermal power. The parameters $P_{t,j}^{CHP}$ and $P_{t,j}^{elec(CHP)}$ are the total power generated by CHP and the electrical power of CHP in each block of linear blocks, respectively. Equation 13 states that the production capacity in each block is between the value before and after it, and the order is observed. $k_{t,j}^{CHP}$ is a binary variable. Equation 14 also states that the output electrical power is taken from only one of the linear block blocks. An Induction furnace is also used to provide a heat profile. The amount of heat generated by this equipment, which uses natural gas as an input, is obtained by equation 15.

$$\mathbf{H^{Furnace}} = \sum_{t=1}^{T} \sum_{l=1}^{N_{furnace}} \gamma_e^{furnace} * P_{t,l}^{gas(input)} \quad (15)$$

For the thermal power generated by CHP, we also have:

$$\mathbf{H^{CHP}} = \sum_{t=1}^{T} \sum_{j=1}^{N_{CHP}} \gamma_g^{CHP} * P_{t,j}^{gas(CHP)} \quad (16)$$

where γ_g^{CHP} is the percentage of heat output produced from the received gas. The cost of starting and shutting it down is also calculated according to Equations 17 and 18.

$$C_{SU}^{CHP} = SU_j^{CHP} * w_t(1 - w_{t-1}) \quad (17)$$

$$C_{SD}^{CHP} = SD_j^{CHP} * w_{t-1}(1 - w_t) \quad (18)$$

In the above equations, SU_j^{CHP} and SD_j^{CHP} are the cost of starting and shutting down CHP in the j block with CHP, respectively. The binary variable w_t also indicates whether CHP is on or off.

$$P^{CHP} - P_A^{CHP} - \frac{P_A^{CHP} - P_B^{CHP}}{H_A^{CHP} - H_B^{CHP}} * (P^{CHP} - P_A^{CHP}) < 0 \quad (19)$$

$$P^{CHP} - P_B^{CHP} - \frac{P_B^{CHP} - P_C^{CHP}}{H_B^{CHP} - H_C^{CHP}} * (P^{CHP} - P_B^{CHP}) > 0 \quad (20)$$

$$P^{CHP} - P_C^{CHP} - \frac{P_C^{CHP} - P_D^{CHP}}{H_C^{CHP} - H_D^{CHP}} * (P^{CHP} - P_C^{CHP}) > 0 \quad (21)$$

Another noteworthy point is that the convex region allowed for CHP operation, due to the dependence of the electrical and thermal power of the output, should only be in the closed environment of figure 2; otherwise, the answers obtained from the problem optimization are wrong and are out of the search space. For this purpose, the CHP performance range can be formulated according to the following equations. The horizontal axis of figure 2 shows the heat output (H^{CHP}), and the vertical axis also shows the electrical output power (P^{CHP}). Equation 19 models all points below the line AB. Equations 20 and 21 include all the points above the BC and CD lines, respectively. The common denominator of this set of triple equations is the allowable performance range of CHP.

2.8. Boiler model

The cost of generating heat by boiler I at hour T and scenario s can be calculated without deducting the maintenance cost of equation 22.

$$cost_{s,i,t}^{boiler} = \frac{H_{s,i,t}}{\eta_{boiler,i}} \pi_{gas,t} \quad (22)$$

In the above equation, $H_{s,i,t}$ shows the thermal power produced by the boiler, $\eta_{boiler,i}$ is its efficiency, and $\pi_{gas,t}$ indicates the price of natural gas.

2.9. Uninterruptible and interruptible loads

Uninterrupted load must always be supplied; almost all the electrical loads are in this category. In order to increase the reliability of the uninterrupted load, in the case of sudden fluctuations in the production capacity of renewable units and load fluctuations, this type of load requires some operational reserve. A short-

term energy storage is required to cope with the power load fluctuations or accommodate the sudden losses in some products. An MG system with many small generators is a flexible system; small generators do not store significant energy in their mechanical inertia, and do not necessarily react quickly to sudden load changes. The operational storage provides the margin of safety for power systems, both small and large, according to the uncertainty of the load and the uncertainty of the output power of renewable energy units for operation with high reliability. In the event of a power outage from the electricity supplier, a large fine must be paid to the consumer. If C_{ls} is considered equal to the average loss due to the interruption of each kwh of load ($/kWh) of this type of load, then the net present value of the loss of this type of load can be obtained according to Equation 23.

$$\mathbf{NPC_{ls} = LOEE\ C_{ls}\ PWA(ir, R)} \quad (23)$$

$\mathrm{PWA(ir, R)}$ is the present value factor of annual payments and LOEE is the Loss of Energy Expectation, which in the next section, their term will be explained. The supply of this type of load does not require operational reserves, and a small percentage of load demand can be the type of interruptible load (similar to cinemas and entertainment centers, etc.). These types of consumers receive money as a reward from the MG manager in a power outage. In other words, the power outage of this type of subscriber does not impose a cost on the MG uninterrupted loads.

2.10. Demand response program (DRP)

Since the consumer response to time-varying rates is not under the network operator's control, the load response provided by time-based applications cannot be selectively controlled and distributed. In contrast, in the distributable load response programs, the system operator can use the response to the load from the customers depending on the conditions and requirements of the system, and include them in the market settlement process. The distributable load response programs include aggregation of load response. In this program, the load response brokers participate in the electricity market as an intermediary between the independent operation of the system and customers. The reduction price is determined based on the agreement of the load and customer response broker. In this model, the load response brokers offer their proposals to the energy market the day before. ISO then implements the recommendations provided by the brokers considering the priorities and features of reducing the burden on customers, launches the load response program, and sends the program information to the participants, and asks them to submit their proposed packages. If these proposals are selected in the market settlement process to be exploited, then the participants should reduce the planned load for the next day. In this work, the operator's performance, demand response, and MG operator are integrated and presented in the microgrid energy management system. In addition to aggregating the load response, the MG energy management system also undertakes its implementation and distribution, thus minimizing the cost of operating MG by using all the potential in MG including loads and production units. If in the modeling DR programs, only a 5% reduction in consumption, then the rate of price reduction will be very significant and about 40%. The sensitivity of load is defined as the ratio of relative changes in load to relative changes in price, according to equation 23. ρ_0 is the initial market price in $/MWh, and q_0 is the initial load valued in MWh.

$$\mathbf{E} = \frac{\partial \mathbf{q}}{\partial \boldsymbol{\rho}} = \frac{\boldsymbol{\rho_0}}{\mathbf{q_0}} \frac{\mathbf{dq}}{\mathbf{dp}} \quad (24)$$

$$\boldsymbol{\xi_{ii}} = \frac{\Delta \mathbf{d}(\mathbf{t_i})}{\Delta \boldsymbol{\rho}(\mathbf{t_i})} \frac{\boldsymbol{\rho_0}}{\mathbf{q_0}}$$
$$\boldsymbol{\xi_{ij}} = \frac{\Delta \mathbf{d}(\mathbf{t_i})}{\Delta \boldsymbol{\rho}(\mathbf{t_j})} \frac{\boldsymbol{\rho_0}}{\mathbf{q_0}} \quad (25)$$

where ρ_0 is the initial market price in $/MWh, and q_0 is the initial demand value in MWh. Self-elasticity (ξ_{ii}) and mutual elasticity (ξ_{ij}) have both positive and negative values, respectively. If the relative change in load is greater than the relative price change, it is called elastic. On the other hand, if the relative change in load is smaller than the relative price change, it is called inelastic. Therefore, the elastic coefficient for one hour of a day can be arranged by a 24-by-24 matrix. The details of the modeling process and formulation of the load response program, which shows how load reduction affects the customer profits, have been reviewed in [23, 24]. In any case, in this work, the corresponding economic response model of the load is presented as (25):

$$\mathbf{d(i)} = \mathbf{d_0(i)} + \sum_{\mathbf{j=1}}^{\mathbf{24}} \mathbf{E_0}\left(\mathbf{i,j}\right). \frac{\mathbf{d_0(j)}}{\boldsymbol{\rho_0(j)}} . \mathbf{A(j)} + \frac{\mathbf{E(i)}\left[\boldsymbol{\rho}\ \mathbf{(i)} - \boldsymbol{\rho_0(i)} + \mathbf{A(i)}\right]}{\boldsymbol{\rho_0(i)}} \quad (26)$$
$$\forall \mathbf{i} = \mathbf{1}, \mathbf{2}, \ldots, \mathbf{24}$$

The above equation shows how much customer load is required to achieve the maximum interest

within 24 hours. This model also includes the price effect at the time of use. Therefore, the following model is used instead:

$$\mathbf{d(i) = d_0(i) + \sum_{j=14}^{18} E_0\left(i,j\right).\ \frac{d_0(j)}{\rho_0(j)}\ .\ A(j)} \quad (27)$$

2.11. DC/AC converter

Not all the renewables manufacturers are synchronous machines. The wind turbines are often induction generators, and the solar units are connected to the system through inverters. The inverters can control the frequency, as the frequency of the inverters can be controlled independently of the load. The DC/AC converter converts the DC electrical power to the AC power at the desired load frequency for load consumption. Its efficiency can model the effect of converter losses.

$$\mathbf{P_{inv-load} = (\sum P_{DG})/\eta_{dc-ac}} \quad (28)$$

2.12. Reliability

Overall, the reliability studies of power systems are divided into long-term (planning) and short-term (operation). The reliability of the generating units is also examined in these two intervals. These studies are called the "static reliability assessment of the production units" in the planning conditions, and the "reliability assessment of the rotating production units" or the "rotating storage units" in the operation conditions. In the static studies, this amount of capacity must respond to the planned outages (maintenance), unplanned (emergency exit), and load growth, while in the conditions of operation, the purpose is to supply the load under emergency exits and uncertainty of the load. The reliability calculations are one of the important issues that should be considered along with the economic and environmental assessments resulting from the distributed generation resources. An accurate evaluation of the economic benefits of using these units requires examining the level of reliability of the systems. The limitation of the available energy from new energy sources and their discontinuous behavior reduces the level of reliability of the system. The authorities have provided several indicators in order to calculate the reliability of the systems including the indicators such as the Loss of Load Expectation (LOLE), Loss of Energy Expectation (LOEE) or Expected Energy Not Supplied (EENS), Loss of Power Supply Probability (LPSP), Equivalent Loss Factor (ELF), and other such cases were mentioned. The above indicators are defined by the following equations [25]. In the above equation, $E\left(LOL(t)\right)$ is the mathematical expectation of disconnection in the time step t that can be defined by equation 29 [25].

$$\mathbf{LOEE = \sum_{t=1}^{N} E\left(LOL(t)\right)} \quad (29)$$

In the above equation, $E\left(LOL(t)\right)$ is the mathematical expectation of disconnection in the time step t that can be defined by equation 30.

$$\mathbf{E\left(LOL(t)\right) = \sum_{s\epsilon S} T_s P_s} \quad (30)$$

In this regard, P_S is the probability of being in the s position, and T_S is the probability of being off load if it is in this position. S is also the total set of possible states for the system.

$$\mathbf{LOEE = EENS = \sum_{t=1}^{N} E\left(LOE(t)\right)} \quad (31)$$

Here, $E\left(LOE(t)\right)$ is the mathematical expectation of the amount of load lost in my time interval, which can be defined by equation 31.

$$\mathbf{E\left(LOE(t)\right) = \sum_{s\epsilon S} Q_s P_s} \quad (32)$$

Where Q_s is the amount of demand lost in terms of (kWh) if it is in the s position.

2.13. Cost of pollution and losses

The cost of pollution and power flow losses in the distribution network will be calculated according to the formulation presented in references [11-16].

3. Objective function

In this section, according to the terms and costs presented in the previous section, the objective function of the problem in equation 32 is explained. The objective function of the problem is to maximize the profit from the sale of battery power or surplus electricity to the grid. The first sentence is the cost or benefit of using the load response programs. The second sentence is the cost of operating the batteries. The third and fourth sentences show the cost of disconnecting the load and the cost of converters and inverters, respectively. In the first sentence of the second line of the objective function, the cost of buying and selling electricity to the upstream network has been announced. Then the costs of the distributed

generation units that are in the network are discussed. The proposed objective function is optimized using the improved frog mutation algorithm, and its method has been given in the next section.

$$O.F. = max \left\{ \begin{array}{l} \sum_{i}\sum_{d}\sum_{r'}[L_{DR}(r,d,t)\Omega(r,d,t)] + \sum_{z}[p_v.N_{bat}.price] + NPC_{ls} + P_{inv-load} \\ + \sum_{t}\left(-\pi_{TOU} \times Load_t + \pi_{sell} \times P_t^{upstream}\right) - \sum_{t}\sum_{i} Cost_{CHP} - Cost_{loss} \\ -\sum_{t}\sum_{k} Cost_{Boiler} - \sum_{t}\sum_{j} Cost_{FC} - \sum_{t}\sum_{r} Cost_{WT} - \sum_{t}\sum_{g} Cost_{PV} - Cost_{Poll} \end{array} \right\} \quad (33)$$

4. Improved Shuffled Frog algorithm

The Shuffled Frog algorithm was first introduced in 2003 by Eusuff and Lansey [26]. In this algorithm, each frog has information about an answer to a problem. The SFLA algorithm contains the initial population of the possible problem answers. These answers are a set of virtual frogs that are themselves divided into several categories. Each group of frogs has characteristics that can change depending on the characteristics of frogs in other groups. SFLA also has a local search that acts like a particle clustering algorithm. For this purpose, the frogs in each group improve their position in relation to food by exchanging information with each other, and after each local search, the information obtained from the groups is compared with each other. In general, the SFLA steps will be as follow:

Step 1: The initial population is randomly generated to the number N_p, and then the fit of the members of this population is determined.

Step 2: The members of the population are arranged in the ascending order based on the fit.

Step 3: The frogs are divided into m groups so that each group contains n frogs. In other words, $N_p = n \times m$. This division should be such that the first frog in the population is assigned to the first group, the second frog to the second group, and the M frog to the M group. Then the frog number m + 1 in the first group and so on, the allocation process continues until n frogs are placed in each one of the m groups.

Step 4: In this step, the local search includes the following steps: we denote the number of categories by m_l. First, m_l is equal to zero, and is compared with the total number of categories (m). The variable y_l also counts the number of local searches. In this step, set y_l to zero, and compare with the maximum local search steps. Therefore, we will have:

$$\mathbf{m_l = m_l + 1} \qquad \mathbf{y_l = y_l + 1} \quad (34)$$

Then for each category, the frog with the best fit and the frog with the worst fit are found, and are named X_b and X_w, respectively. The position of the best fit among all frogs is also called X_g. The position of the frogs is then improved using the following equation, as shown in figure 3:

$$\mathbf{D_i = rand \times (X_b - X_w)} \qquad \mathbf{X_w^{new} = X_w^{old} + D_i} \quad (35)$$

where *rand* is a random number between 0 and 1. Given that $-D_{max} < D_i < D_{max}$, D_{max} will indicate the maximum change in the position of the frogs. If a better frog (better answer) is obtained during this stage, it will be replaced with the previous frogs; otherwise, in equation 19, X_g is used instead of X_b, and the above steps will be repeated, and if a better answer is obtained, replaces the previous answer; otherwise, a frog is randomly generated and replaced with the previous frog.

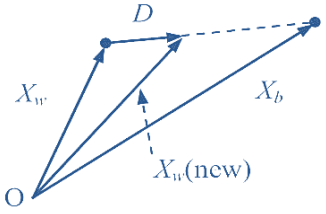

Figure 3. How to create a new path for frogs.

If $m_l < m$, $m_l = m_l + 1$ must be replaced, and if $y_l < y_{max}$, $y_l = y_l + 1$ must be replaced; otherwise, we will return to the second step.

Step 5: If the convergence conditions are not achieved, the search process is repeated from step 3; otherwise, the algorithm is stopped, and the best answer is considered as the output. In order to improve the frog jump algorithm, it should be noted that the classical SFLA algorithm is placed along the X_b and X_w lines when the frogs with the worst fit strengthen their position relative to the group or the best frog. This may lead the algorithm to the wrong answers. For this reason, a way to improve this algorithm is introduced. The main idea of this method is to expand the direction and length of each frog's jump, thus preventing the algorithm from converging incorrectly.

In this method, if the first four frogs are randomly selected among the arranged frogs in such a way that relation (36) is established, then the change of the position of the frogs is selected as relation (37).

$$\mathbf{X_{g1} \neq X_{g2} \neq X_{g3} \neq X_{g4}} \tag{36}$$

$$\mathbf{X_{change} = X_{g1} + r_1(X_{g2} - X_{g3}) + r_2(X_g - X_{g4})}$$

$$\mathbf{X_{w,j}^{new}} = \begin{cases} \mathbf{X_{change}} & \mathbf{if\ r_3 < r_4\ \ or\ \ j = r_p} \\ \mathbf{X_g} & \mathbf{otherwise} \end{cases} \tag{37}$$

where t represents the number of iterations of the category, and r_p is a random number between 1 and the number of categories. The variables $r_1, r_2, r_3, and\ r_4$ are all random numbers between zero and 1. If this improvement leads to a better answer, it replaces the previous answer; otherwise, a random answer is generated and replaces the previous answer.

5. Simulation and analysis of results

This section deals with the case simulations in the standard 69-bus and 118-bus IEEE networks. It should be noted that the details of the power generation of the units are given in the 69-bus IEEE network, and in the other two networks, it will be enough to provide the results only. Figure 4 shows the amount of electrical and thermal power required on a given day in the 69-bus network. The price of electricity purchased from the upstream network as well as the cost of natural gas consumption is also shown in figures 5 and 6 [29].

In the ISFLA algorithm, the initial population value is 50 frogs. The program is performed in the MATLAB software using a system with Windows 7 specifications, GB4 RAM, and CPU core i7, which is performed in 100 replications. First, the power generation range of the production units is shown in table 1, and the convergence diagram for the first scenario (base scenario) is shown in figure 7.

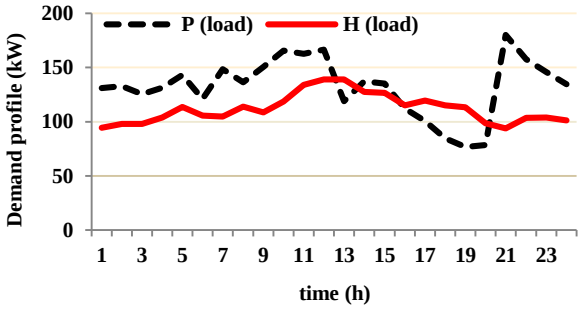

Figure 4. Electrical and thermal charge profile of MG.

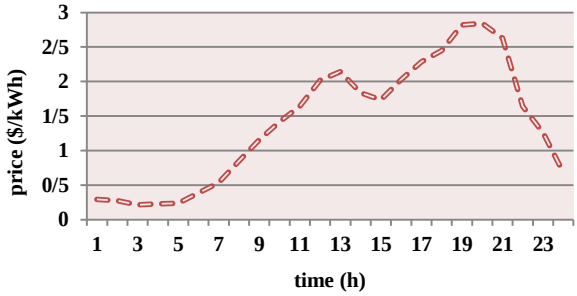

Figure 5. Electricity price chart with ToU tariff.

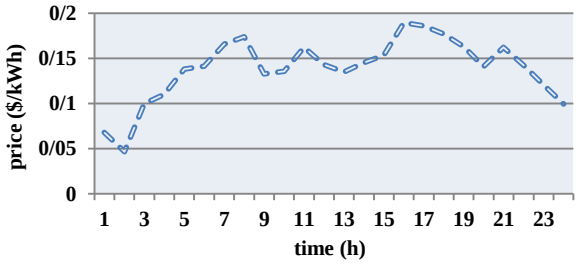

Figure 6. Gas price chart.

Table 1. Production capacity range of units.

DG type	Capacity [kW] (min, max)	price $/kWh]	Start up/ shut sown costs	CO_2 [kg/MWh]
FC	(20, 60)	0.752	2.68	703.52
PV	(0, 50)	0.704	-	-
Boiler	(10, 100)	0.423	1.82	83.35
Wind	(0, 80)	3.015	-	-
CHP	(25,65)	1.572	2.57	301.45

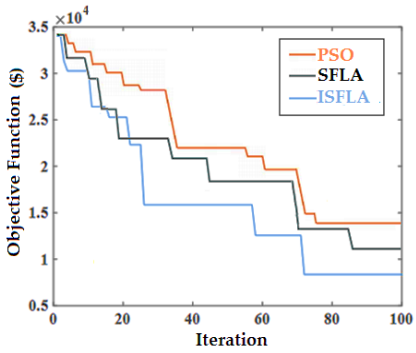

Figure 7. Convergence diagram of the objective function in the first scenario by the proposed ISFLA algorithm.

In these simulations, four scenarios are presented, as follow:

- Optimization of the objective function with the same weight coefficients (1/3) on the amount of pollution, losses, and DRP.
- Optimization of the objective function with a weight coefficient of 50% for DRP and a weight coefficient of 25% for both losses and pollution.
- Optimization of the objective function with a weight coefficient of 50% for pollution and a weight coefficient of 25% for both losses and DRP.
- Optimization of the objective function with a weight coefficient of 50% for losses and a weight coefficient of 25% for both pollution and DRP.

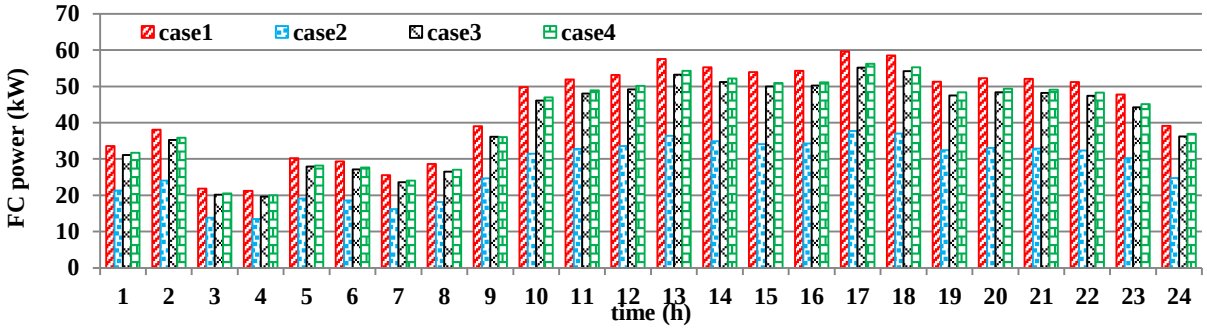

Figure 8. Production capacity of fuel cell in all four case studies.

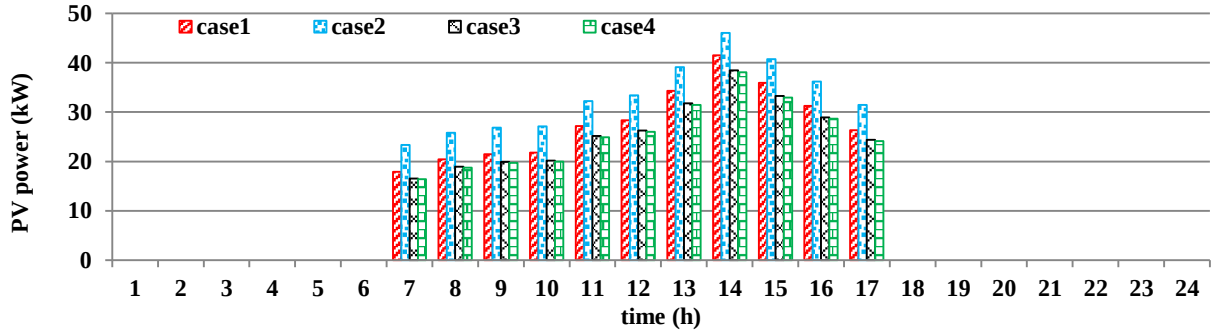

Figure 9. Amount of photovoltaic power generation in all four case studies.

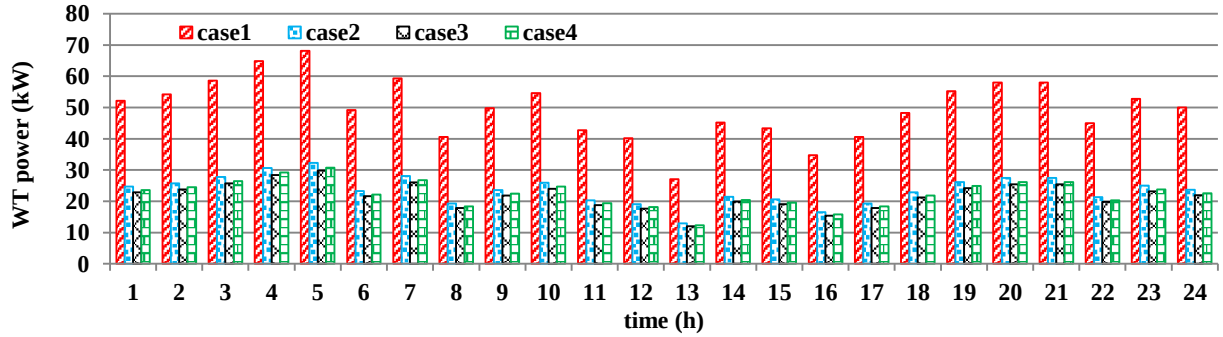

Figure 10. Production capacity of wind turbines in all four case studies.

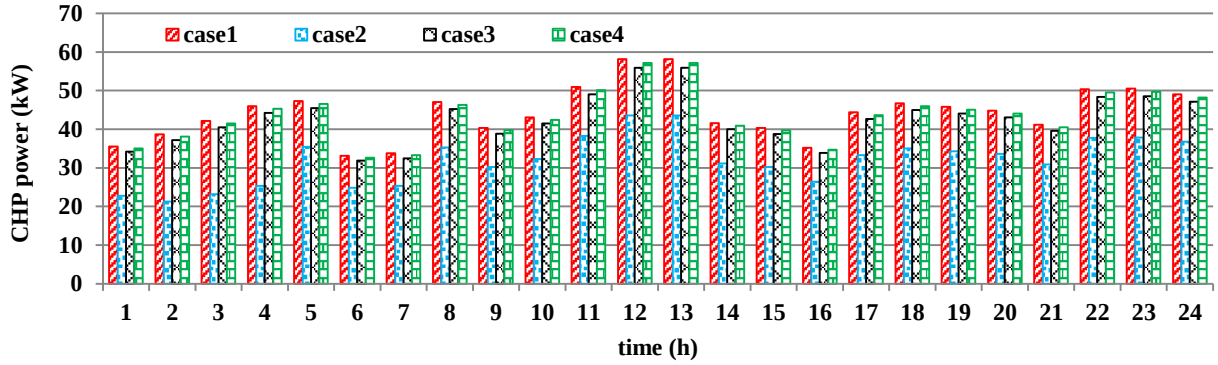

Figure 11. Production capacity of CHP in all four case studies.

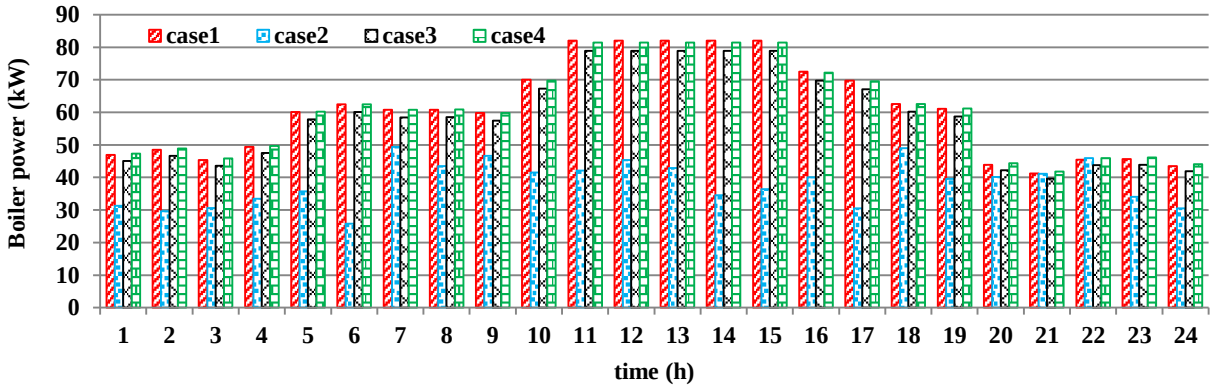

Figure 12. Amount of boiler production capacity in all four case studies.

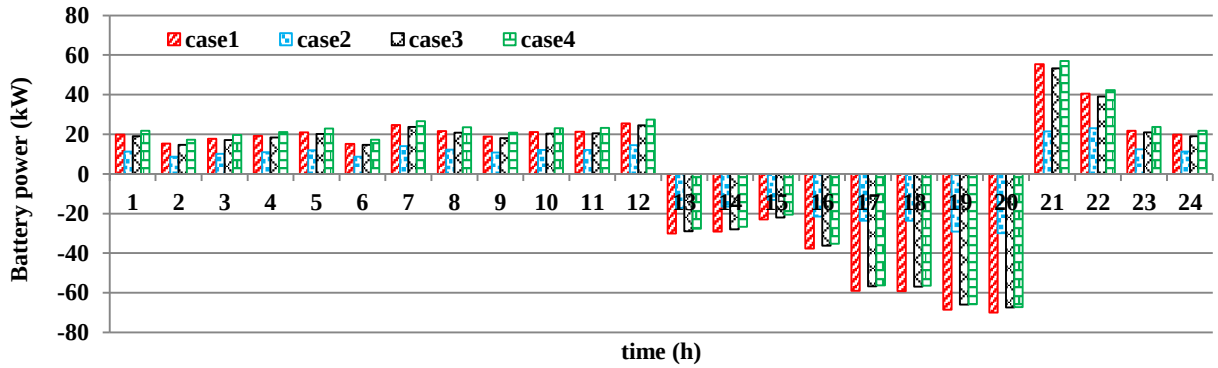

Figure 13. Battery participation capacity in all four case studies.

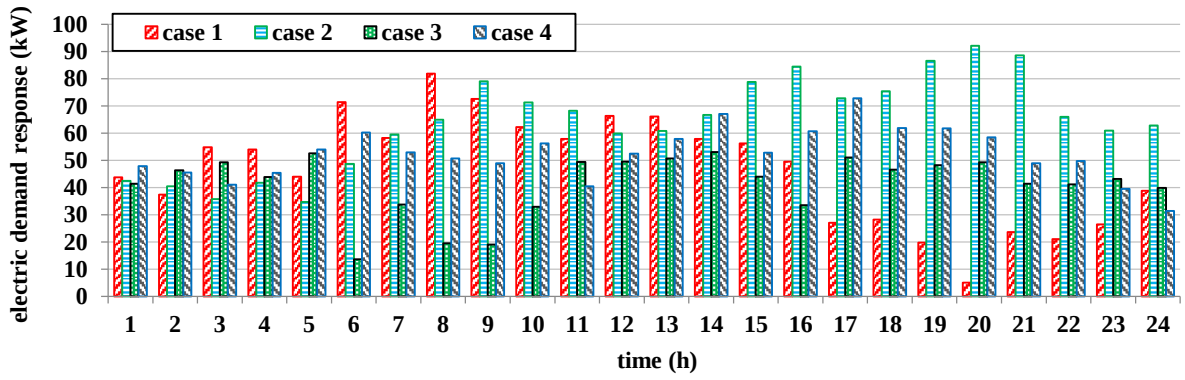

Figure 14. Level of participation of DRP programs in reducing electrical demand.

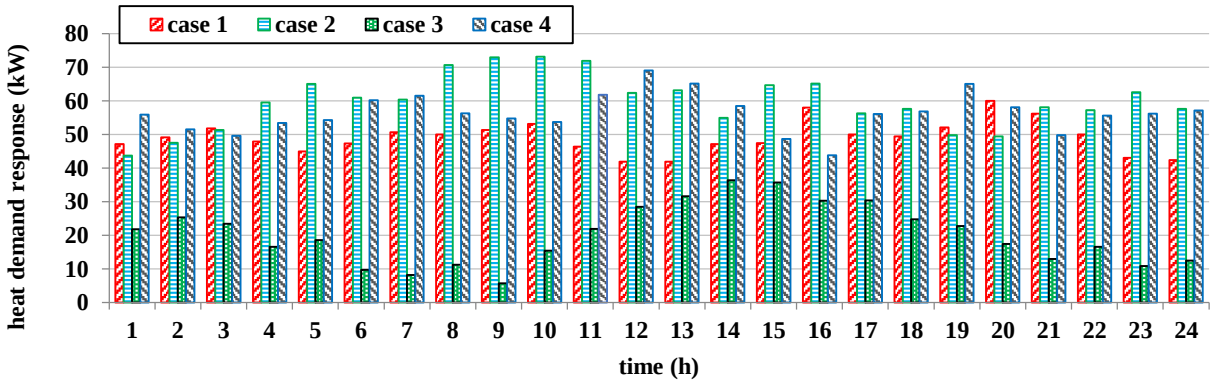

Figure 15. Level of participation of DRP programs in reducing thermal demand.

6. Discussion

In the first scenario, given that the pollution, network losses, and DRPs are observed equally, this scenario can be considered as a baseline, and other case studies can be evaluated according to Scenario 1. The operating costs, in this case, are estimated at $3,250, with DR programs reducing the electrical and thermal demand costs by 12.7% and 8.5%, respectively. In the second scenario, the weight of minimizing operating costs increases due to the increase in profits from the use of DRP. The output of the improved frog jump algorithm is estimated to cost $2,675, with a reduction in the electricity and heating costs of 19.9% and 14.3%, respectively. In this case, the consumer participation in the operation has reached its maximum. In the third scenario, the weight reduction of pollution caused by fossil fuels in CHP and boiler, and most of the other provisions will be the subject, will bring the operating costs in 2859 dollars. In this case, the amount of electricity and heat savings according to DRP programs are 8.4% and 6.6%, respectively. Finally, in the fourth scenario, with the increase in the impact of losses, the operating cost reaches $2,968, and the DR programs have a positive effect of 10.9% and 7.8% on the supply of electrical and thermal demand, respectively.

Figures 8 to 12 illustrate the capacities generated by distributed generation sources in the studied scenarios. It is observed that most of the thermal power is supplied by the boiler, and only 20% of it is supplied by CHP. In figure 13, the impact of participation in the battery energy management program is well-described. The battery is discharged during the peak hours and charges during low hours. The degree of participation of the DRP programs in all four scenarios is also shown in figures 14 and 15.

Table 2. Comparison of loss and pollution costs in the studied scenarios

Costs	Case 4	Case 3	Case 2	Case 1
Loss	108.5 $	158.1 $	123.9 $	175.5 $
Pollution	108.9 $	82.3 $	102.5 $	103.2 $

Table 3. Optimal arrangement of DERs in IEEE 69-bus network

DERs		FC	PV	WT	CHP	Boiler
Case 1	Numbers	4	4	1	2	2
	Bus No.	45-51-61-34	36-50-54-63	21	12-36	33-21
Case 2	Numbers	2	2	1	2	2
	Bus No.	26-33	61-40	14	8-28	44-6
Case 3	Numbers	3	3	2	3	3
	Bus No.	69-47-43	32-48-5	23-40	50-34-16	19-38
Case 4	Numbers	3	2	3	2	2
	Bus No.	28-14-49	61-10	26-7-41	44-9	54-21

Table 4. Optimal arrangement of DERs in IEEE 118-bus network

DERs		FC	PV	WT	CHP	Boiler
Case 1	Numbers	5	7	3	2	4
	Bus No.	17-24-50-92-117	8-9-26-84-87-104-112	38-56-70	46-80	22-45-32-106
Case 2	Numbers	3	4	3	2	3
	Bus No.	8-24-87	15-50-71-98	39-59-117	6-90	15-72-109
Case	Numbers	5	6	4	3	4

3	Bus No.	5-23-49-83-108	13-23-56-86-95-115	12-44-80-104	35-69-102	20-48-68-107
Case 4	Numbers	4	5	3	2	3
	Bus No.	8-24-50-117	9-15-71-95-116	38-59-104	45-91	23-45-108

Table 5. Comparison of reliability index with existing algorithms.

Index	PSO [27]	SFLA [26]	TLBO [28]	Proposed
LOEE	25.3%	18.3%	16.7%	11.2 $
ELF	23.6%	21.9%	19.8%	16.2%

Table 6. Comparison of different costs with existing algorithms.

Total casts	PSO [27]	SFLA [26]	TLBO [28]	Proposed
Mean voltage profile	0.991 pu	0.967 pu	0.974 pu	1.013 pu
Mean pollution costs	244.284 $	286.542 $	255.491 $	212.974 $
Mean loss costs	371.512 $	399.476 $	384.597 $	349.122 $
Operation costs	3425 $	3512 $	3309 $	3190 $
Benefits using DRP	972 $	655 $	786 $	989 $

The degree of reliability calculated by the proposed algorithm and their comparison with the existing algorithms are given in Table 5. It is observed that both the supplied energy is in the lowest possible state, and the definite demand index is lower than the other methods. Finally, Table 6 compares the output cost results and voltage profiles using the ISELA algorithm and the particle swarm method, ordinary frog jump, and TLBO. It is observed that in the proposed method, the voltage profile is in a more favorable condition than the others; the operating cost is minimized and the profit from participating in the DRP programs is reached to the maximum.

7. Conclusion

In this paper, an optimization method based on a SFLA was presented with the aim of finding the optimal solution for energy management in a MG considering different approaches. The objective function considered in this work included the pollution and loss costs, battery participation, and operating costs, the output results of which showed the best arrangement for the desired number of DER. According to the case studies, it was observed that during the low-consumption hours, energy was purchased at a cheap price from the upstream network and stored in the battery, and thus during the peak hours, in addition to providing the required power to the MG demands, an additional energy upstream network was sold to increase the revenue. The results of the case studies focused on an average of 16.5% and 10.6% reduction in the total operating costs of losses and reduction of pollution, respectively. Considering the demand response plans could also reduce the operating costs by up to 24%, and was profitable for the customers. The upstream network (diesel generator) and boiler pollutions that changed the design of the network were not negligible. Finally, the best arrangement for the various IEEE standard MGs was selected, which were arranged to supply both heat and electricity at the same time. The results obtained and their comparison with the other methods showed that the profits of using DRP increased, while the operating cost decreased. The definitive demand reduction and LOEE reduction also increased the reliability of the proposed method. The most important advantage of using the proposal was finding the optimal answers in the shortest possible time and the highest accuracy compared to the existing optimization methods. Furthermore, using ISELA, the operating costs were significantly reduced.

8. Reference

[1] R. Alayi and H. Rouhi, "Techno-Economic analysis of electrical energy generation from Urban waste IN HAMADAN, IRAN," International Journal of Design and Nature and Ecodynamics, Vol. 15, No. 3, pp. 337–341, 2020.

[2] R. Alayi and J. Javad Velayti, "Modeling/optimization and effect of environmental variables on energy production based on PV/wind TURBINE hybrid system," Jurnal Ilmiah Teknik Elektro Komputer dan Informatika, Vol. 7, No. 1, p. 101, 2021.

[3] A. Kasaeian, A. Shamel, and R. Alayi, "Simulation and economic optimization of wind turbines and photovoltaic hybrid system with storage battery and hydrogen tank (case study the city of Yazd)" Journal of

current research in science, Vol. 3, No. 5, pp. 96-105, 2021.

[4] H. Khalili, A. Arash, and R. Alayi, “Simulation and economical optimization hybrid system PV and grid in Ardabil city” Journal of Current Research in Science, Vol. 3, No. 5, pp. 74-83, 2015.

[5] R. Alayi and F. Jahanbin, “Generation management analysis of a stand-alone photovoltaic system with battery” Renewable Energy Research and Application, Vol. 1, No. 2, pp. 205-209, 2020.

[6] R. Alayi, M.R. Basir Khan, and M.S. Mohmammadi, “Feasibility study Of GRID-CONNECTED PV system for peak demand reduction of a residential building in Tehran, Iran,” Mathematical Modelling of Engineering Problems, Vol. 7, No. 4, pp. 563–567, 2020.

[7] M. Parvania, and M. Fotuhi-Firuzabad. "Demand Response Scheduling by Stochastic SCUC." IEEE Transactions on Smart Grid, Vol. 1, No. 1, 2010.

[8] C.S. Ioakimidis, L.J. Oliveira, and K.N. Genikomsakis, "Wind power forecasting in a residential location as part of the energy box management decision tool", IEEE Transactions on Industrial Informatics, Vol. 10, No. 4, pp. 2103-2111, 2014.

[9] D.T. Nguyen, M. Negnevitsky, and M.D. Groot, "Walrasian market clearing for demand response exchange", IEEE Transactions on Power Systems, Vol. 27, No. 1, pp. 535-544, 2012.

[10] M. Moreno, M. Bueno, and J. Usaola, "Evaluating risk-constrained bidding strategies in adjustment spot markets for wind power producers", International Journal of Electric Power and Energy System, Vol. 43, pp. 703-711, 2012.

[11] E. Bitar, R. Rajagopal, P. Khargonekar, K. Poolla, and P. Varaiya, "Bringing wind energy to market", IEEE Transactions on Power Systems, Vol. 27, No. 3, pp. 1225-1235, 2012.

[12] L. Baringo and A.J. Conejo, "Strategic offering for a wind power producer", IEEE Transactions on Power Systems, Vol. 28, No. 4, pp. 4645-4654, 2013.

[13] M. Zugno, J.M. Morales, P. Pinson, and H. Madsen, "Pool strategy of a price-maker wind power producer", IEEE Transactions on Power Systems, Vol. 28, No. 3, pp. 3440-3450, 2013.

[14] A.A.S. de la Nieta, J. Contreras, J.I. Munoz, and M. O’Malley, "Modeling the impact of a wind power producer as a price-maker", IEEE Transactions on Power Systems, Vol. 29, No. 6, pp. 2723-2732, 2014.

[15] E. Heydarian-Forushani, M. Moghaddam, M. Sheikh-El-Eslami, M. Shafie-khah, and J. Catalao, "Risk-constrained offering strategy of wind power producers considering intraday demand response exchange", IEEE Transactions on Sustainable Energy, Vol. 5, No. 4, pp. 1036-1047, 2014.

[16] S. Chua-Liang and D. Kirschen, "Quantifying the effect of demand response on electricity markets", IEEE Transactions on Power Systems, Vol. 24, No. 3, pp. 1199-1207, 2009.

[17] H.M. Hasanien, "Shuffled Frog Leaping Algorithm for Photovoltaic Model Identification," in IEEE Transactions on Sustainable Energy, Vol. 6, No. 2, pp. 509-515, April 2015.

[18] S. Alaee, R. Hooshmand, and R. Hemmati, "Stochastic transmission expansion planning incorporating reliability solved using SFLA meta-heuristic optimization technique," in CSEE Journal of Power and Energy Systems, Vol. 2, No. 2, pp. 79-86, June 2016.

[19] W. Ding, Y. Sun, L. Ren, H. Ju, Z. Feng, and M. Li, "Multiple Lesions Detection of Fundus Images Based on Convolution Neural Network Algorithm With Improved SFLA," in IEEE Access, Vol. 8, pp. 97618-97631, 2020

[20] M. Shafie-khah, P., Moghaddam, and M.K. Sheikh-El-Eslami, "Unified solution of a non-convex SCUC problem using combination of modified branch-and-bound method with quadratic programming", Energy Conversion and Management, Vol. 52, pp. 3425-3432, 2011

[21] R. Karki, P. Hu, and R. Billinton, "A simplified wind power generation model for reliability evaluation", IEEE Trans. Energy Convers., Vol. 21, No. 2, pp. 533-540, 2006

[22] L. Vandezande , L. Meeus , R. Belmans , M. Saguan, and J.M. Glachant, "Well-functioning balancing markets: A prerequisitefor wind power integration", Energy Policy, Vol. 38, pp. 3146-3154, 2010

[23] J.A. Guimãraes, L.M.V.G. Pinto, and N. Maculan, "What will be the proxy value for a Brazilian utility company triggering its demand side management in the light of price elasticity of demand?," in IEEE Latin America Transactions, Vol. 14, No. 8, pp. 3746-3754, Aug. 2016.

[24] A. Mnatsakanyan and S.W. Kennedy, "A Novel Demand Response Model with an Application for a Virtual Power Plant," in IEEE Transactions on Smart Grid, Vol. 6, No. 1, pp. 230-237, Jan. 2015.

[25] D. Elmakias, Ed. New computational methods in power system reliability. Vol. 111. Springer Science and Business Media, 2008.

[26] M. Eusuff and K. Lansey. "Optimization of water distribution network design using the shuffled frog leaping algorithm." Journal of Water Resources planning and management 129, No. 3, pp. 210-225, 2003.

[27] A.C. Pérez-Flores, J.D.M. Antonio, V.H. Olivares-Peregrino, H.R. Jiménez-Grajales, A. Claudio-Sánchez, and G.V.G. Ramírez, "Microgrid Energy Management With Asynchronous Decentralized Particle Swarm

Optimization," in IEEE Access, Vol. 9, pp. 69588-69600, 2021.

[28] M.J.H. Moghaddam, A. Kalam, S.A. Nowdeh, A. Ahmadi, M. Babanezhad, and S. Saha,"Optimal sizing and energy management of stand-alone hybrid photovoltaic/wind system based on hydrogen storage considering LOEE and LOLE reliability indices using flower pollination algorithm," in Renewable energy, Vol. 135, pp. 1412-1434, 2019.

[29] V.R. VC, Optimal renewable resources placement in distribution networks by combined power loss index and whale optimization algorithms. Journal of Electrical Systems and Information Technology, Vol. 5, No. 2, pp. 175-191, 2018.